Vibrational Energy Transfer and Heat Conduction in a Protein

Xin Yu and David M. Leitner*

Department of Chemistry and Chemical Physics Program, University of Nevada, Reno, Nevada 89557

Received: July 8, 2002; In Final Form: September 23, 2002

The normal modes of myoglobin, their lifetimes, the speed of sound, and mean free path are calculated to determine the coefficient of thermal conductivity and thermal diffusivity for the protein. A propensity is found for frequency differences of pairs of normal modes localized to nearby regions of the protein to be several hundred cm^{-1}. As a result, the anharmonic decay rate of higher frequency, localized normal modes, calculated by perturbation theory, is typically nearly independent of temperature, consistent with results of pump−probe studies on myoglobin. The thermal diffusivity of myoglobin at 300 K is calculated to be 14 $Å^2$ ps^{-1}, the same as the value for water. The thermal conductivity at 300 K is found to be 2.0 mW cm^{-1} K^{-1}, about one-third the value for water.

1. Introduction

Anharmonic decay of vibrational modes in the amide I band of globular proteins occurs in about 1 ps,[1−3] a time that is essentially independent of temperature from below 10 K to over 300 K.[3] Atoms oscillating with appreciable amplitude in a given vibrational mode of the amide I band, which ranges from about 1600 to 1700 cm^{-1}, span a limited region of the protein backbone. Indeed, already at far lower frequencies, starting from around 150 cm^{-1}, the normal modes of proteins are localized to particular segments of the molecule.[4−8] At physiological temperatures, a significant fraction of thermally accessible vibrational modes are therefore localized. Because proteins generally function in only fairly narrow temperature ranges, it is vital that excess heat produced in a reaction be transported efficiently. Because a large fraction of thermally accessible modes are localized, they cannot carry heat without anharmonic transfer of energy to other modes. To transport heat efficiently, anharmonic decay of vibrational modes of a protein should be rapid over a significant range of temperatures, and the observed lifetimes in the amide I band indicate this to be the case, at least at these rather high frequencies.

In this paper, we calculate the coefficient of thermal conductivity and thermal diffusivity for myoglobin based on the normal modes, the speed of sound in the protein, mean free path, localization length, and energy transfer rates among the normal modes. The speed of sound, which is found to be 23 Å ps^{-1} at low frequency, is calculated by matching low frequency modes of the protein to the nearest plane wave in three-dimensional space. The mean free path is estimated as the correlation length of the direction of atomic displacements in normal modes. The rate of anharmonic decay of normal modes is calculated by perturbation theory in terms of low-order anharmonic coupling of the modes. We assume, then, that the protein oscillates around a local minimum in the potential, and thereby focus on vibrational dynamics in a given configuration of the protein. Below the glass transition temperature of about 200 K, conformational changes are slow and vibrations alone account for thermal transport. We assume that vibrations largely account for heat conduction at higher temperatures, too. Because our focus is on vibrational energy transport and heat conduction in the protein alone, we consider for now the protein free of any solvent molecules.

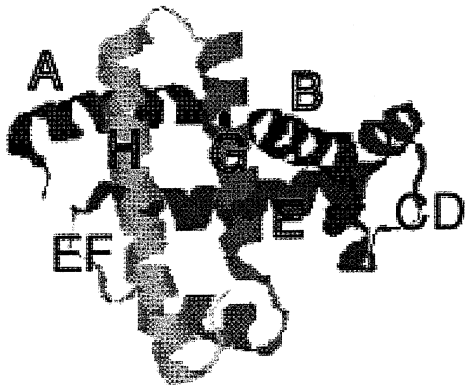

Figure 1. Ribbon diagram of sperm whale myoglobin. The five largest α helices of myoglobin, labeled A, B, E, G, and H, and the two largest coil segments, labeled CD and EF, are indicated in the figure for reference to earlier work.

Normal modes of globular proteins have been calculated for some two decades, and a clear picture of the extent of atomic displacements in normal modes as a function of frequency has long emerged.[4−8] Anharmonic matrix elements coupling some of the normal modes of bovine pancreatic trypsin inhibitor[9] and myoglobin[10] have also been calculated. Here, we report calculations of the lifetimes of normal modes of myoglobin. We have recently calculated the anharmonic decay rates of the normal modes of helical and coil segments of myoglobin consisting of 10−24 amino acids.[11,12] The structure of myoglobin is shown in Figure 1, and the five largest α helices and two largest coil segments which were studied are indicated there. One striking property of the normal modes of both proteins and these peptide sequences is the extent of spatial localization, the onset of which occurs below 200 cm^{-1}, with atomic displacements usually increasingly restricted with higher frequency. In this respect, the vibrations of proteins resemble those of one-dimensional (1D) glasses,[13−15] for which almost all normal modes are localized; only at low frequency are the normal modes extended over a finite, 1D disordered object. In contrast, most vibrational

* To whom correspondence should be addressed. E-mail: dml@chem.unr.edu.

10.1021/jp026462b CCC: $25.00
Published on Web 01/22/2003

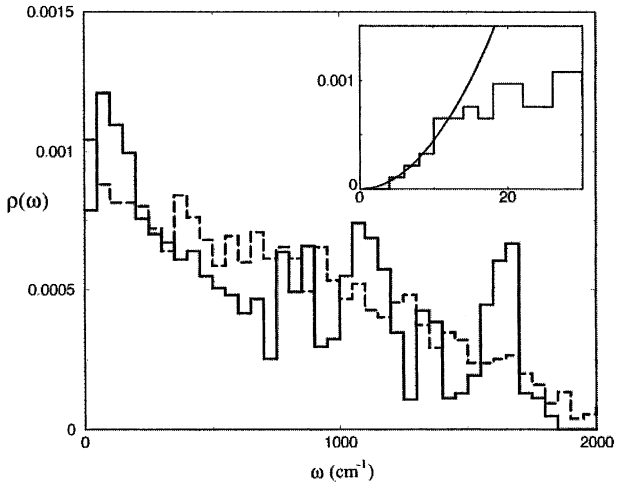

Figure 2. Normalized distribution of normal-mode frequencies, $\rho(\omega)$, binned into 50 cm^{-1} intervals, of myoglobin (solid line) and a 1D glass model discussed in the text (dashed line). The insert shows $\rho(\omega)$ for the protein at small ω and a fit to $\rho(\omega) \propto \omega^2$ up to $\omega \approx 12$ cm^{-1}.

modes of proteins are quite different from those of 3D glasses. For the latter, only a relatively small fraction of modes at the upper band edge are spatially localized; the large majority are extended over the object.[16−18] Energy transfer from most vibrational modes of both proteins and 1D glasses occurs by anharmonic decay, which is restricted to modes that are resonantly coupled, and is fastest for modes that overlap in space.[10−12] We incorporate the role of anharmonic decay in heat transfer in proteins by adopting an anharmonically induced hopping model that has been used to calculate the contribution of energy transfer from localized modes to thermal conduction in glasses.[15,19,20]

In the following section, we present computational results for the normal modes of myoglobin. We discuss the extent to which residues of the protein participate in a normal mode, the propensity for nearby localized modes to have widely spaced frequencies, as well as the speed of sound in myoglobin, and the mean free path. In section 3, lifetimes of the normal modes are calculated and discussed, in particular the temperature dependence of the lifetimes of spatially localized modes. Section 4 presents calculations of the thermal conductivity and thermal diffusivity of myoglobin. Concluding remarks follow in section 5.

2. Normal Modes

2.1. Myoglobin. Computation of the normal modes was carried out using the program package MOIL, which was written by Elber and co-workers.[21] Coordinates for the atoms in myoglobin were taken initially from the Protein Data Bank entry, and the new minimum energy structure was subsequently computed. The final structure was obtained when the norm of the gradient was 0.002 kcal mol^{-1} $Å^{-1}$, and the normal modes for this structure were then calculated. The number of atoms in the calculation is 1543 and the number of normal modes is 4623. The normal modes of the protein span a frequency range from 5 to 1842 cm^{-1} and then a higher range from 3054 to 3712 cm^{-1}. The high-frequency modes above 3000 cm^{-1} corresponding to CH, NH, and OH stretches will not be considered here, as their contribution to thermal transport is negligible. Figure 2 shows the density of normal modes of myoglobin as a function of mode frequency. Up to about 12 cm^{-1}, $\rho(\omega)$ appears to vary as ω^2 and so follows a Debye relation for a three-dimensional object at very low frequency. The mode density is highest at fairly low frequency, 50−100 cm^{-1}, and it declines with substantial fluctuations as the frequency increases to the band edge of about 1850 cm^{-1}.

In describing the normal modes of a protein, it is instructive to compare them with those of a simple model of a polymer, such as a chain of atoms, both periodic and aperiodic. In a harmonic periodic chain, the normal modes carry energy without resistance from one end of the 1D crystal to the other. On the other hand, the vast majority of normal modes of an aperiodic chain are spatially localized and cannot carry heat. A protein molecule, which is of course not periodic, can be better characterized as an aperiodic chain of atoms, and most normal modes of a protein are likewise localized in space. If a normal mode α is exponentially localized, then the amplitude of oscillation of atoms in mode α decays from the center of excitation, $\mathbf{R}_0$, as

$$|\mathbf{e}_\alpha(\mathbf{R}_n)| \propto \exp(-|\mathbf{R}_n - \mathbf{R}_0|/\xi) \quad (1)$$

where $|\mathbf{e}_\alpha(\mathbf{R}_n)|$ is the magnitude of the displacement of atom n, located at $\mathbf{R}_n$; ξ is the localization length; and $\mathbf{R}_0$ is the position of the atom overlapping the largest component of the normal mode vector. To determine ξ, we calculate $\ln|\mathbf{e}_\alpha(\mathbf{R}_n)|$ for all atoms and plot it against $|\mathbf{R}_n - \mathbf{R}_0|$. Results for $\ln|\mathbf{e}_\alpha(\mathbf{R}_n)|$ vs $|\mathbf{R}_n - \mathbf{R}_0|$ averaged over normal modes in 50 cm^{-1} intervals between 300 and 350 cm^{-1} are shown in Figure 3(a). A best fit gives $\xi = 7.24$ Å. We also plot in the same figure $\ln|\mathbf{e}_\alpha(\mathbf{R}_n)|$ vs $|\mathbf{R}_n - \mathbf{R}_0|$ for the normal modes in the ranges 550−600 and 950−1000 cm^{-1}. Best fits give, respectively, $\xi = 4.61$ and 2.91 Å. In this way, we have calculated ξ for all of the normal modes of myoglobin in 50 cm^{-1} intervals and plotted the results in Figure 3b. At sufficiently low frequency, below about 150 cm^{-1}, the normal modes appear to be essentially delocalized over the protein, with $\xi \approx 16-17$ Å, comparable to the radius of myoglobin. Above 150 cm^{-1}, ξ decreases to values between 2.5 and 5 Å, corresponding to lengths of some 1 to 4 bonds.

A number of other useful measures of localization in proteins have been suggested and calculated, most common among them the participation number,[22] an estimate for the number of atoms in a protein that participate in a normal mode. Similarly, we can determine the extent to which a normal mode spans the protein residues.[11,12] As a measure of the number of residues contributing to a mode, we calculate the information entropy

$$S_\alpha = -\sum_{i=1}^{N_{res}} p_i \ln p_i \quad (2)$$

where N_{res} is the total number of residues in the protein and p_i is the projection of all coordinates of a residue onto normal mode α of the protein. If vibrations of each residue contribute equally to this normal mode then $S_\alpha = \ln N_{res}$, whereas $S_\alpha = 0$ if a normal mode vibration is localized to a single residue. Then e^S is comparable to the number of residues that a normal mode spans. The value of e^S for myoglobin versus normal-mode frequency is plotted in Figure 4, where we have averaged e^S over modes in 50 cm^{-1} intervals. Overall, the qualitative variation of e^S with ω mimics that of ξ with ω in Figure 3b. We also plot in Figure 4 the average value of e^S for the five largest helices of myoglobin[12] for comparison. We observe in both cases that the number of residues contributing to a mode generally declines with increasing mode frequency, and their values are similar above 500 cm^{-1}. For myoglobin, the largest value of e^S is 96, corresponding to about two-thirds the number of residues that make up the protein. In this frequency range,

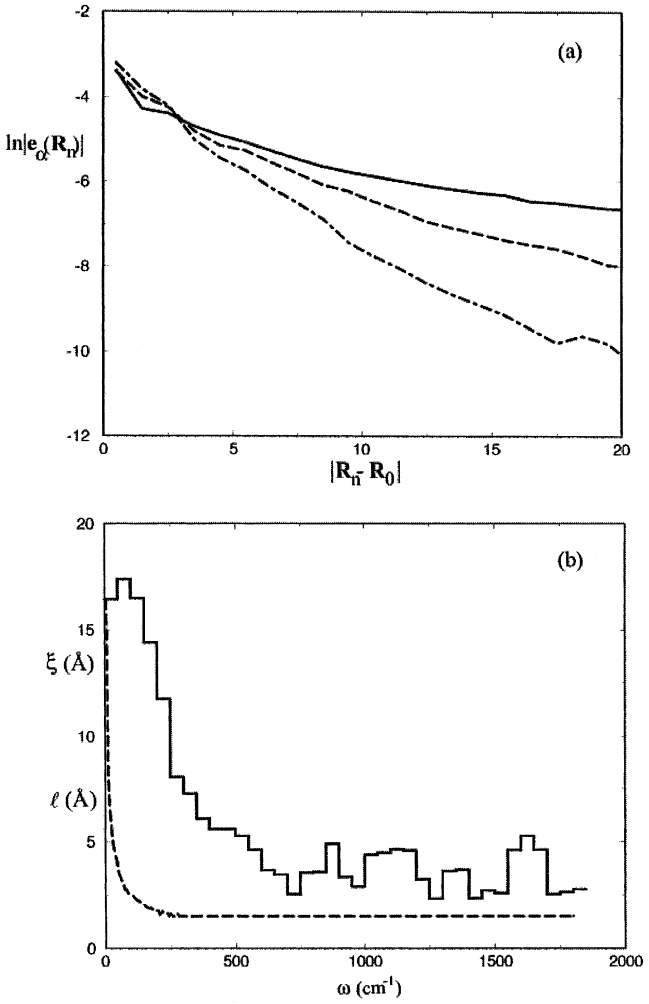

Figure 3. (a) Localization length, ξ, defined by eq 1 is obtained from the slope of $\ln|\mathbf{e}_\alpha(\mathbf{R}_n)|$ vs $|\mathbf{R}_n - \mathbf{R}_0|$, which is plotted after averaging over normal modes in intervals between 300 and 350 cm^{-1} (solid), 550−600 cm^{-1} (dashes), and 950−1000 cm^{-1} (dot−dashes). Best fits give, respectively, $\xi = 7.24$, $\xi = 4.61$, and $\xi = 2.91$ Å. (b) Localization length, ξ, (solid) and mean free path, ℓ, (dashes) averaged over 50 cm^{-1} intervals.

the normal modes are essentially extended over the protein, just as we saw by inspecting the localization lengths above. We also found in our calculation of e^S for the five largest α helices of myoglobin that its value approaches about two-thirds the total number of residues at low frequency, where the normal modes are extended. As seen in Figure 4, at frequencies below about 200 cm^{-1}, the largest value of e^S is 12, or about two-thirds of the on average 19 residues that comprise the helices.

2.2. Localized Modes of Myoglobin and 1D Glasses. The large majority of normal modes of myoglobin are spatially localized. As such, the vibrations of proteins have much in common with those of 1D disordered systems. Perhaps the simplest such system is a chain of atoms, each connected to its nearest-neighbor by a random force. For such a one-dimensional "glass", only the very lowest-frequency modes are extended over the chain, similar to the case for a protein. We consider such a glass where the force constant that couples nearest-neighbor atoms is selected randomly from a distribution parametrized to mimic that of proteins, a model introduced in refs 11 and 12 to compare with modes of the helices of myoglobin. We reintroduce the model here simply to illustrate one important consequence of strong localization of normal modes, namely, that frequencies of normal modes whose localization centers overlap

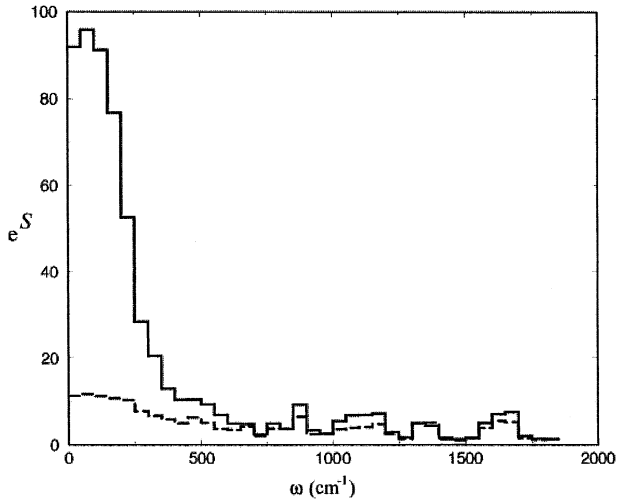

Figure 4. Value of e^S, a measure of the number of amino acids that participate in a normal mode vibration, binned into 50 cm^{-1} intervals is plotted as a function of frequency for myoglobin (solid line). The dashed line is the average value of e^S for the five largest α helices of myoglobin.

in space are generally very different. This trend, as discussed in this section, gives the appearance of "repulsion" of mode frequencies between pairs of nearby localized modes. Consider, for instance, just two oscillators vibrating with frequencies ω_1 and ω_2. If the oscillators are near one another in space, they are coupled to each other by perhaps several hundred cm^{-1}, whereas if they are far apart, the coupling between them is small. For the vibrational energy to remain localized in one oscillator, the difference in their frequencies, $|\omega_1 - \omega_2|$, must be several hundred cm^{-1} if the oscillators are close in space, whereas there is no such restriction if they are far apart. Such mode repulsion has important consequences on the temperature dependence of the anharmonic decay rates of normal modes of proteins, as will be discussed section 3.

Our model for a 1D glass is a chain of N equally spaced atoms of unit mass connected by random forces. For the calculations discussed here, we take an ensemble of five chains of $N = 500$ atoms. The potential energy of the glass is simply

$$V = \frac{1}{2}\sum_{n=1}^{N} f_n (u_n - u_{n+1})^2 \qquad (3)$$

with u_n the displacement of atom n from equilibrium and f_n the force constant. (Because we express frequencies in cm^{-1}, it will be convenient to express f_n in units of (cm^{-1})^2.) The normal-mode frequencies are obtained from the eigenvalues of the Hessian matrix, whose diagonal elements are $d_n = f_{n-1} + f_n$. By contrast, the diagonal elements, d, of the Hessian matrix for a protein are the sums of numerous terms accounting for a larger number of local interactions. We have found, however, that vibrational properties of the simple chain model can mimic vibrational properties of proteins given an appropriate distribution of force constants. As a simple model, discussed in detail elsewhere,[12] we take the force constants, f_n, to be randomly distributed in an exponential distribution such that the standard deviation of the distribution of $d_n = f_{n-1} + f_n$, the diagonal elements of the Hessian of the model, matches that for myoglobin. For the latter, we have found a standard deviation of 9.5×10^5 (cm^{-1})^2. We have also modified the exponential distribution for f_n by introducing a large-f_n cutoff of 1.7×10^6 (cm^{-1})^2 to prevent mode frequencies much higher than the band

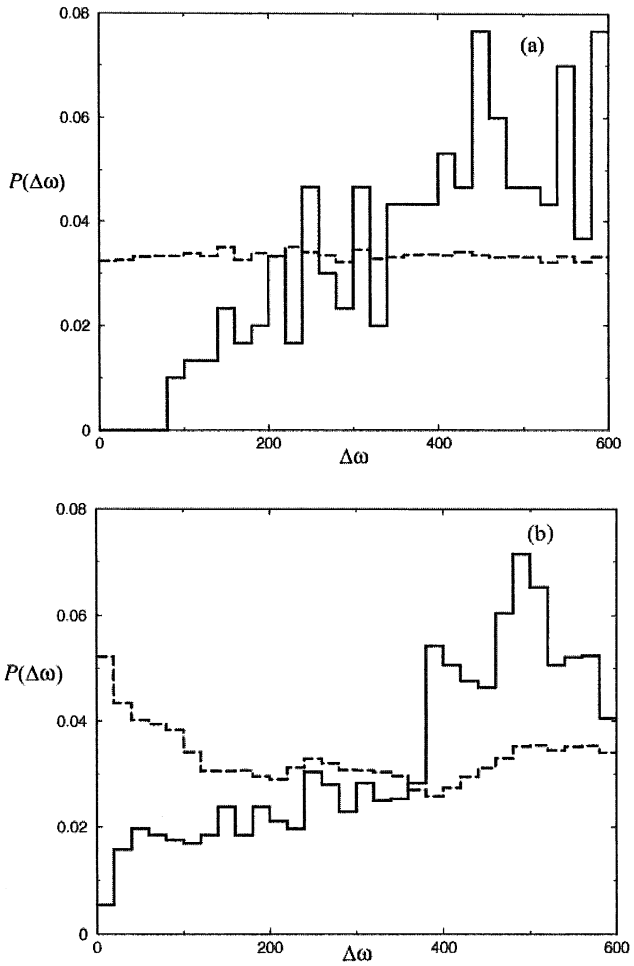

Figure 5. Probability, $P(\Delta\omega)$, of finding a pair of vibrational modes with frequency difference $\Delta\omega$ in (a) the 1D glass model and (b) myoglobin, when at least one of the modes is localized with frequency ω in the range 1000 cm^{-1} < ω < 2000 cm^{-1}. Dashed lines are probabilities for any pair of modes with frequency difference $\Delta\omega$, regardless of their distance from one another in space. The solid lines are results only for vibrational modes that lie near one another in space. In (a), they correspond to vibrational modes whose maximum components lie over nearest-neighbor atoms in the 1D glass. In (b), the pairs of eigenstates are restricted to those whose largest components lie within 2 Å of each other in myoglobin.

edge for myoglobin. Then f_n is taken randomly from an exponential distribution with standard deviation 4.0×10^5 (cm^{-1})^2 and cutoff 1.7×10^6 (cm^{-1})^2. In Figure 2, we compare the normal mode density of the harmonic 1D glass consisting of 5 chains with $N = 500$ with the normal mode density of myoglobin. The secular variation of the mode density of myoglobin with mode frequency reveals specific features reflecting its constituents and interactions. Nevertheless, these features appear as fluctuations around the mode density of the model. We point out that there is nothing very special about the particular force constant distribution that we have chosen; the distribution of force constants that we use simply sets the scale of the frequencies and density of vibrations to be comparable to that of myoglobin.

The influence of spatial localization of two normal modes in the 1D glass and in myoglobin on the frequency difference of these vibrational modes is shown in Figure 5. We locate the largest component of each normal mode, α, and calculate the probability, $P(\Delta\omega)$, that for another mode, β, whose largest component lies a certain distance away from the largest component of mode α, the difference in frequency between the two modes is $\Delta\omega = |\omega_\alpha - \omega_\beta|$. We consider only localized modes, α, whose frequency, ω_α, falls between 1000 and 2000 cm^{-1}. Probabilities are calculated for $\Delta\omega$ in intervals of 20 cm^{-1} up to $\Delta\omega = 600$ cm^{-1}. Results for the 1D glass are shown in Figure 5a and results for myoglobin in Figure 5b. The dashed histograms in both (a) and (b) are averages over all pairs of normal modes, regardless of the distance between the largest components of modes α and β.

Consider first the 1D glass shown in (a). For any pair of modes α and β, there is just as much chance that the difference between their vibrational frequencies is small, say, less than 100 cm^{-1}, as it is fairly large, 500−600 cm^{-1}. The solid-line histogram gives the probability of finding $\Delta\omega$ when the maximum component of eigenstates α and β are on nearest-neighbor atoms of the glass. In this case, we find no pairs of modes with $\Delta\omega \leq 80$ cm^{-1} and about half as many as found on average for any distance between the modes when $\Delta\omega$ is between about 100 and 200 cm^{-1}. Instead, larger values of $\Delta\omega$, closer to 500 or 600 cm^{-1}, are expected to be found when normal modes α and β are localized to neighboring atoms. We thus observe for the 1D glass that vibrational modes localized close to one another in space tend to have frequencies that are quite different. Turning to (b), we see the same pattern for the normal modes of myoglobin. The dashed line again gives the probability of finding modes whose frequency difference is $\Delta\omega$ for all pairs of modes, with one member of the pair a localized mode such that 1000 cm^{-1} < ω < 2000 cm^{-1}. In this case, when we can ignore the distance of the modes from one another, there is generally a somewhat larger chance of finding pairs of modes whose frequency difference is small, below about 100 cm^{-1}. However, if we only consider pairs of modes whose largest components overlap atoms that lie less than 2 Å from each other, we obtain the solid-line histogram in (b). As for the 1D glass, we see that if pairs of localized modes lie close in space, there is a propensity for their frequency differences to be large, in this case around 500 cm^{-1}, rather than small, say, below 200 cm^{-1}. Such a propensity diminishes as we consider localized normal modes whose largest components lie farther away from each other. For distances between 4 and 5 Å, as well as larger distances, we find $P(\Delta\omega)$ to be essentially the same as the dashed histogram, for which the distance between the localization centers of the modes is ignored.

2.3. Correlation of Direction of Atomic Displacements in Normal Modes. For normal-mode frequencies below about 150 cm^{-1}, atomic oscillations are extended over the protein. Nevertheless, although the motions of the atoms appear collective at these low frequencies, the rate of energy transport depends on the extent to which the direction of motion of the atoms is correlated. Our analysis of this correlation follows that of Nishikawa and Go,[4] who considered the low-frequency modes of bovine pancreatic trypsin inhibitor. The correlation functions for the direction of atomic displacements that we compute for myoglobin are quite similar to theirs. By comparing the correlation function with that for a plane wave in three-dimensional space, we can extract a wavenumber for a low-frequency mode and thereby estimate the speed of sound in myoglobin. Our main aim in calculating correlations in the direction of atomic displacements is to determine a frequency-dependent correlation length, which we adopt to estimate the mean free path for sound waves in a protein, because this is the distance over which an excitation propagates in a particular direction. Beyond the correlation length, directions of atomic displacements appear random.

Consider normal mode α. We can define a direction vector of displacement for an atom, n, whose position is $\mathbf{R}_n$ at the potential minimum as $\mathbf{A}_\alpha(\mathbf{R}_n) = \mathbf{e}_\alpha(\mathbf{R}_n)/|\mathbf{e}_\alpha(\mathbf{R}_n)|$. The correlation function for the direction vector of two atoms spaced a distance $d = |\mathbf{R}_n - \mathbf{R}_{n'}|$ apart is then[4]

$$C_\alpha(d) = \frac{\sum_n \sum_{n'} \mathbf{A}_\alpha(\mathbf{R}_n)\cdot\mathbf{A}_\alpha(\mathbf{R}_{n'})\delta(d - |\mathbf{R}_n - \mathbf{R}_{n'}|)}{\sum_n \sum_{n'} \delta(d - |\mathbf{R}_n - \mathbf{R}_{n'}|)} \quad (4)$$

The correlation function $C_\alpha(d)$ is thereby defined as an average over dot products of direction vectors of displacements of pairs of atoms separated in space by distance d. At very low frequency, vibrations of proteins behave like those in a continuous three-dimensional space. For example, we observe in Figure 2 that the density of normal modes follows a Debye relation for a 3D bulk object at frequencies below 15 cm^{-1}. It is therefore of interest to compare $C_\alpha(d)$ for the low-frequency normal modes of myoglobin with the corresponding correlation function for a plane wave in three dimensions. The latter is given by[4]

$$C_P(d) = (-1)^{k+1}[k(k+1)\lambda/2d + 2d/\lambda - (2k+1)] \quad (5)$$

where λ is the wavelength of the plane wave, and k is the integral part of $2d/\lambda$.

In Figure 6 parts a−c, we plot $C_\alpha(d)$ for three normal modes with frequencies 10.0, 15.0, and 50.0 cm^{-1}, respectively. The equivalent result for a plane wave, $C_P(d)$, decays from 1 to 0 at a distance d that is half the wavelength of the plane wave and then becomes negative and returns to 0 at a value of $d = \lambda$. We can fit the results for $C_\alpha(d)$ to the nearest plane wave result by matching the lowest d where $C_\alpha(d) = 0$ with $\lambda/2$ of the plane wave. The results, $C_P(d)$, for the corresponding plane waves are also plotted in Figure 6, where for ω = 10.0, 15.0, and 50.0 cm^{-1} we use for the plane wave λ = 32, 21, and 12 Å, respectively. For the normal mode with frequency 10.0 cm^{-1}, we find that the corresponding plane wave with λ = 32 Å fits the result for $C_\alpha(d)$ quite well out to the largest d, 40 Å, where we could calculate $C_\alpha(d)$. The same is true of all of the normal modes below 11.7 cm^{-1}, or the lowest 12 modes. At higher frequency, however, $C_\alpha(d)$ no longer looks like $C_P(d)$. For instance, at ω = 15.0 cm^{-1}, we see that $C_\alpha(d)$ decays to 0 followed at larger d by only small fluctuations around 0 compared to the oscillations for the nearest plane wave; variation of C_α with d also appears more random than following an oscillation with wavelength λ. By ω = 50.0 cm^{-1}, shown in Figure 6c, fluctuations about 0 following the initial decay of $C_\alpha(d)$ are very small and appear mostly as noise. Normal modes with frequencies as low as 15 cm^{-1} already seem to be composed of several if not many plane waves, and their atomic displacement vectors appear partly incoherent. As a result, $C_\alpha(d)$ decays to 0 and essentially remains at 0 for larger d. The decay of $C_\alpha(d)$ allows us to estimate the mean free path of a sound wave, which we consider in section 4.

Using the correlation function $C_\alpha(d)$ and matching it to $C_P(d)$, where possible, allows us to determine the speed of the plane wave corresponding to normal mode α. We determine first the lowest value of d where $C_\alpha(d) = 0$, which is $\lambda/2$ for the corresponding plane wave. The wavenumber is $k = 1/\lambda$. If we plot ω vs k, the slope gives us the speed of sound in the protein, $c_s = \partial\omega/\partial k$. In general, ω is a nonlinear function of k, and the value of c_s depends on the range of modes we consider.

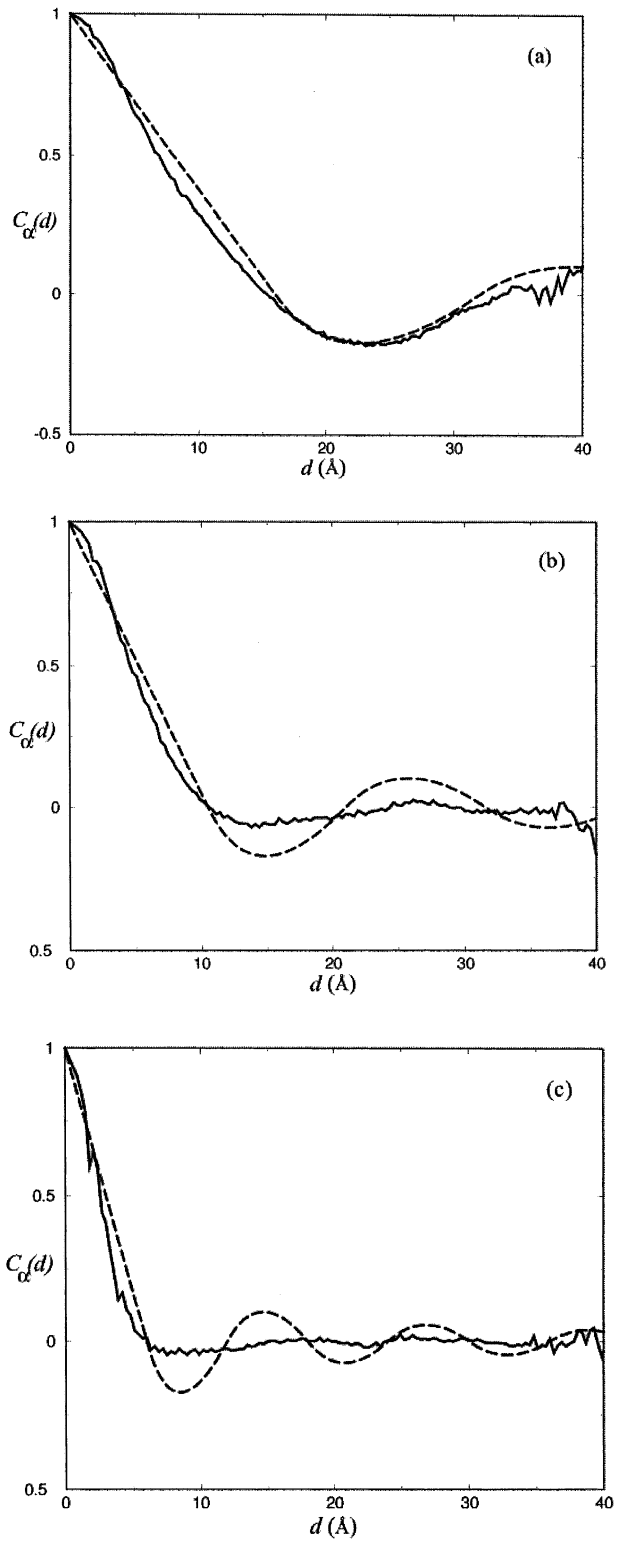

Figure 6. Correlation function for the direction vector of two atoms spaced by d, $C_\alpha(d)$, defined by eq 4, is plotted for three normal modes of myoglobin. The smoother, oscillatory curve plotted alongside is the result, $C_P(d)$, given by eq 5, for the closest plane wave. $C_\alpha(d)$ for modes with frequencies of 10.0, 15.0, and 50.0 cm^{-1}, are plotted in (a), (b), and (c), respectively. $C_P(d)$ for plane waves with λ = 32, 21, and 12 Å are plotted in (a), (b), and (c), respectively.

In Figure 7, we plot ω (in units of ωc, where c = 0.03 cm ps^{-1}) vs k (= $1/\lambda$), where λ is found from $C_\alpha(d)$, for the normal modes from 5 to about 35 cm^{-1}. Linear regression through the points in the plot yields c_s = 22.8 Å ps^{-1} for this range of low-frequency modes.

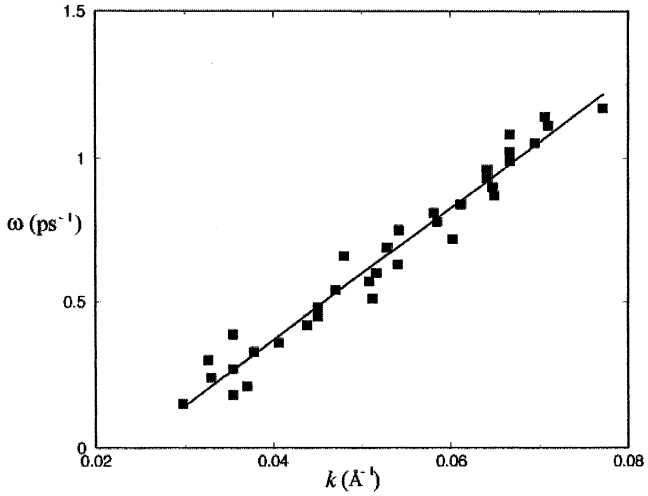

Figure 7. Frequency, ω, is plotted against wavenumber, k, where the latter is determined by matching $C_\alpha(d)$, defined by eq 4, for all normal modes of myoglobin up to 40 cm^{-1}, with $C_P(d)$, given by eq 5 for the nearest plane wave. The slope of the line that best fits the data gives for the speed of sound $c_s = 22.8$ Å ps^{-1}.

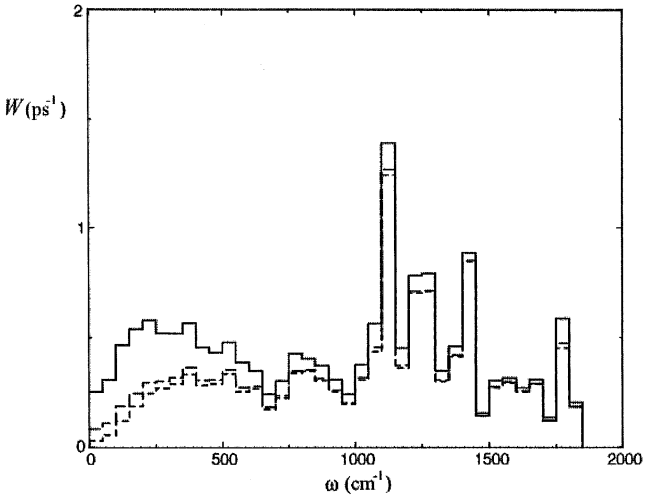

Figure 8. Anharmonic decay rates, W, of the normal modes of myoglobin are plotted as a function of mode frequency, ω, at 15 (short dashes), 45 (long dashes), and 135 K (solid line).

3. Anharmonic Decay Rates

We turn now to the lifetimes of the normal modes. In our calculation of energy transfer rates we consider only the contribution of cubic anharmonic terms in the potential energy of myoglobin, which is valid if we consider sufficiently low temperatures. The energy transfer rate from mode α, W_α, can then be written as a sum of terms that can be described as decay and collision[23]

$$W_\alpha^{\text{decay}} = (\hbar\pi/8\omega_\alpha)\sum_{\beta,\gamma}(|\Phi_{\alpha\beta\gamma}|^2/\omega_\beta\omega_\gamma)(1 + n_\beta + n_\gamma)\delta(\omega_\alpha - \omega_\beta - \omega_\gamma) \quad (6a)$$

$$W_\alpha^{\text{coll}} = (\hbar\pi/4\omega_\alpha)\sum_{\beta,\gamma}(|\Phi_{\alpha\beta\gamma}|^2/\omega_\beta\omega_\gamma)(n_\beta - n_\gamma)\delta(\omega_\alpha + \omega_\beta - \omega_\gamma) \quad (6b)$$

where n_α is the occupation number of mode α, which at temperature T we take to be

$$n_\alpha = (e^{\hbar\omega_\alpha/k_BT} - 1)^{-1} \quad (7)$$

The matrix elements $\Phi_{\alpha\beta\gamma}$ appear as the coefficients of the cubic terms in the expansion of the interatomic potential in normal coordinates, computed numerically as

$$\Phi_{\alpha\beta\gamma} = (\partial^2V/\partial Q_\alpha\partial Q_\beta|_{Q_0+\delta Q_\gamma} - \partial^2V/\partial Q_\alpha\partial Q_\beta|_{Q_0-\delta Q_\gamma})/2\delta Q_\gamma \quad (8)$$

where Q_α is a mass-weighted normal coordinate and Q_0 is the equilibrium position of the protein in normal coordinates. At low temperatures, the energy transfer rate is dominated by processes that involve the decay of a vibrational excitation into two others, and decay terms dominate for energy transfer from most modes at higher temperatures, too. We shall assume throughout that $W_\alpha \approx W_\alpha^{\text{decay}}$, so that the energy transfer rate, W_α, from mode α is given by eq 6a. The most serious error in this approximation, which should be small at the temperatures we consider, occurs at low frequency, a regime where the normal modes are anyway extended over the protein.

In Figure 8, we plot the anharmonic decay rate for myoglobin as a function of frequency at 15, 45, and 135 K. Particularly noteworthy is that the vibrational energy transfer rates are not very sensitive to temperature above about 500 cm^{-1}. Significant temperature dependence of the anharmonic decay rate implies that energy is flowing directly into the low-frequency modes of myoglobin. As mode frequency increases, the transfer rate apparently becomes less dependent on temperature; there is thus little direct energy transfer from high-frequency to low-frequency modes. This suggests that matrix elements coupling a given high-frequency mode to a pair of other modes are small if the frequency of one of the pair is small. For energy transfer to occur at all, the frequency of the given high-frequency mode must be the sum of frequencies into which energy is transferred. For the matrix element coupling this triple of modes to be appreciable, the three modes must also overlap in space.

As mode frequency increases, the normal mode vibrations generally become more localized. A given high-frequency mode, α, is therefore strongly spatially localized. If its energy decays to a low-frequency mode of the protein, the rest of the energy must decay into a localized mode whose frequency must be similar to ω_α. However, we have seen in section 2 that localized modes close in space tend to "repel" one another; localized modes with similar frequencies rarely overlap in space. As a consequence, energy transfer to a localized mode with similar frequency and the remainder to low-frequency modes occurs very slowly. The anharmonic decay rate from high-frequency modes is then only weakly temperature dependent.

Temperature-independent anharmonic decay rates of high-frequency modes of myoglobin have been observed in time-resolved spectroscopic studies. Pump−probe vibrational spectra of the amide I band, between 1600 and 1700 cm^{-1}, from 6 to 310 K by Peterson et al. revealed decay rates from about 0.5 to 1 ps^{-1},[3] slightly faster but similar to the values we calculated. Over this sizable temperature range the decay rate remained the same to within a factor of 2. Similarly, pump−probe studies by Fayer, Dlott, and co-workers[24,25] on myoglobin−CO found that the decay of the CO stretch with a frequency of about 1950 cm^{-1} is also essentially independent of temperature over the same temperature range. In this case, part of the reason for the very weak temperature dependence is due to the fact that the CO stretch frequency lies some 100 cm^{-1} above the band of protein vibrational frequencies.

We mention that the anharmonic decay rates in myoglobin are generally similar to the average decay rates in the five largest α helices of myoglobin as well as the two coil segments

indicated in Figure 1. The average decay rate of normal modes up to 1850 cm^{-1} is about 0.3 ps^{-1} for myoglobin, just under 0.6 ps^{-1} for the helices,[12] and about 0.2 ps^{-1} for the coil segments.[12] The somewhat faster average decay rate in the helices is partly due to a few especially high anharmonic decay rates that were calculated for specific modes in some of the helices, as detailed in ref 12. The specific resonances that give rise to these small number of fast decay rates in the individual helices are apparently absent in the protein. Overall, the variation of the anharmonic decay rate with mode frequency in myoglobin and in the peptide segments is the same, as well as the dependence of the rate on temperature. These general trends were mimicked by the 1D glass model presented in section 2.2 with the introduction of cubic anharmonicity to the glass model using an appropriate relation between the cubic anharmonic constants and force constants.[12]

4. Thermal Conduction in Myoglobin

In this section, we assemble the information that we have gained about the normal modes of myoglobin and their lifetimes in sections 2 and 3 to describe the flow of heat in this protein. We calculate the coefficient of thermal conductivity, which relates the net energy flux to the thermal gradient, defined by

$$\kappa = \int \mathrm{d}\omega\, n(\omega)\, C(\omega)\, D(\omega) \tag{9}$$

where $n(\omega)$ is the density of states, $C(\omega)$ the heat capacity per unit volume, and $D(\omega)$ the frequency-dependent energy diffusion coefficient. The thermal diffusivity is defined by

$$D_T = \frac{\kappa}{\int \mathrm{d}\omega\, n(\omega)\, C(\omega)} \tag{10}$$

where the denominator is the heat capacity per unit volume at temperature T

$$n(\omega) = \rho(\omega) N \tag{11}$$

$$C(\omega) = \frac{\hbar^2\omega^2}{V k_B T^2} \frac{\exp(\hbar\omega/k_B T)}{[\exp(\hbar\omega/k_B T) - 1]^2} \tag{12}$$

where $\rho(\omega)$ is the normalized density of states plotted in Figure 2; N is the total number of vibrational modes, which is 4348 (up to 1850 cm^{-1}); T is temperature; k_B is Boltzmann's constant; and V is the volume of the protein. We are assuming that the heat capacity of myoglobin is a function only of its vibrational energy. To estimate the volume of myoglobin, we assume for simplicity that the protein is a sphere with radius 17 Å. The number of atoms increases as the square of the radius out to 15 Å; there are still atoms beyond this distance, but their number rapidly decreases with increasing radius. If the volume density of these remaining atoms were the same as that up to a radius of 15 Å, the total volume would be a sphere of radius 17 Å, so we choose the latter as our estimate for the volume of myoglobin.

To calculate the coefficient of thermal conductivity and thermal diffusivity, we need to estimate the frequency-dependent energy diffusion coefficient, $D(\omega)$. We begin by considering the vibrational modes in the normal mode limit. In this case, $D(\omega)$ can only be defined for the extended modes, where $\omega <$ 150 cm^{-1}, in which case

$$D_h(\omega) = \frac{1}{3} c_s(\omega) l(\omega) \tag{13}$$

where c_s is the speed of sound, l the mean free path, and the subscript h refers to the harmonic, normal mode limit. The mean free path, $l(\omega)$, can extend upward to a characteristic length of the protein, say, 20 Å, down to a typical interatomic spacing of roughly 1.5 Å. In section 2, we found the speed of sound in myoglobin to be $c_s = 23$ Å ps^{-1} for $\omega \approx 20$ cm^{-1}. Because ω varies nonlinearly with k, the value for c_s depends on mode frequency. For instance, we find $c_s \approx 27$ Å ps^{-1} for $\omega \approx 50$ cm^{-1}. However, for this range of ω and higher, it becomes increasingly difficult to assign a meaningful value of k, so that c_s becomes difficult to estimate. We shall therefore use $c_s = 23$ Å ps^{-1} throughout. We obtain the mean free path, $l(\omega)$, from the correlation of the direction of atomic displacements as a function of distance between atoms calculated in section 2. Other than at very low frequencies, up to about 11 cm^{-1}, for which the mean free path appears to be about the length of the protein, the correlation $C(d)$ decays rapidly with increasing d followed by only weak fluctuations at larger d. There thus appears to be a characteristic distance up to which the direction of atomic displacements remains correlated and beyond which any correlation is essentially lost. An excitation can thereby propagate this distance before it would appear randomly reoriented in the protein. We estimate the mean free path, $l(\omega)$, to be the decay length of $C(d)$, which we take to be the distance, d, at which $C(d) = 1/e$. A different estimate is needed for the lowest dozen or so modes in myoglobin, for which a plane wave appears to be an adequate description. For these very low-frequency modes, a more appropriate estimate for $l(\omega)$ is perhaps the diameter of the protein, though which value we use for these few modes has very little influence on our estimates for the thermal conductivity and diffusivity.

The mean free path, $l(\omega)$, as a function of ω is plotted in Figure 3b together with the localization length of the normal modes. The mean free path should not be smaller than a bond length, and we use as a representative value for a bond length 1.3 Å, which is the average distance between nearest-neighbor atoms at the local minimum. The minimum mean free path is reached for modes with $\omega >$ 200 cm^{-1}, near the crossover from extended to localized normal modes. Using the values of $l(\omega)$ plotted in Figure 3b, together with $c_s = 23$ Å ps^{-1} calculated in section 2, we can estimate the frequency-dependent diffusion coefficient in the harmonic limit using eq 13. We then calculate the coefficient of thermal conductivity in the harmonic limit as

$$\kappa_h(T) = \int_0^{\omega_l} \mathrm{d}\omega\, n(\omega)\, C(\omega)\, D_h(\omega) \tag{14}$$

where we use $\omega_l = 150$ cm^{-1} as the upper limit, above which the normal modes are localized. Our result for κ_h is plotted in Figure 9a as a dashed curve for temperatures from 20 to 320 K. This is the thermal conductivity of myoglobin in the harmonic limit, where only the independent normal modes can carry heat. We observe that κ_h increases with T until $T \approx 100$ K, at which point it begins to saturate, increasing with T only slowly in approaching its limiting value of about 1.2 mW cm^{-1} K^{-1}.

We consider now the influence of the localized normal modes, with frequencies greater than about 150 cm^{-1}, on heat transport in the protein. If the normal modes of myoglobin were not localized above 150 cm^{-1}, κ_h could be calculated by integrating eq 14 over the entire band of frequencies, where the mean free path, $l(\omega)$, would be typically a bond length. In this case, the thermal conductivity would continue to increase with temperature far above 100 K. This is illustrated in Figure 9a with the upper, dot−dashed curve, which corresponds to κ_h calculated using as an upper limit for the frequency the upper band edge

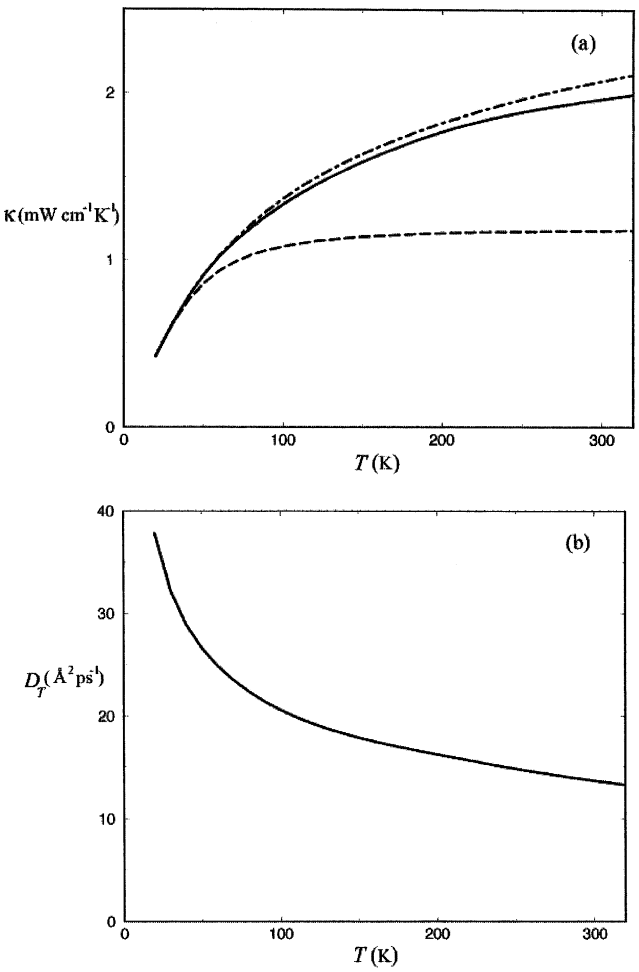

Figure 9. Coefficient of thermal conductivity calculated for myoglobin from $T = 20-320$ K is plotted as a solid curve in (a). The dashed curve gives the thermal conductivity if no anharmonic coupling of normal modes is included in the calculation. The dot−dashed curve gives, for reference, the coefficient of thermal conductivity for myoglobin if all normal modes were extended over the protein. (b) Thermal diffusivity calculated for myoglobin is plotted from 20 to 320 K.

of 1850 cm^{-1}. Localization apparently reduces the thermal conductivity by almost a factor of 2 at $T \approx 300$ K in the harmonic limit.

Though the normal modes above 150 cm^{-1} are localized, anharmonicity gives rise to finite lifetimes of the normal modes, which we have seen to be on the order of 1−10 ps for these modes. Energy localized to a normal mode is transferred to other modes on this time scale. To estimate the role of anharmonicity in thermal diffusion, we adopt a hopping model used to describe energy transfer among localized modes of glasses.[15,19,20] If, near a given frequency, the localization length has a typical value $\xi(\omega)$, then energy can diffuse this distance before a transition to other modes takes place. If the anharmonic transition rate, $W(\omega)$, is sufficiently slow, then $\xi(\omega)$ is effectively the distance over which energy spreads in a time $W^{-1}(\omega)$. The mean free path is then the localization length, ξ, and the time before energy can transfer elsewhere is the mode lifetime, W^{-1}. The diffusion coefficient due to anharmonic transitions is then

$$D_a(\omega) \approx \frac{1}{3}\xi^2(\omega)\, W(\omega) \tag{15}$$

where the subscript a indicates energy transfer because of anharmonic coupling of normal modes. If, however, $W^{-1}(\omega)$ is sufficiently short, then a vibrational excitation will not have spread as far as $\xi(\omega)$ before a transition to other modes takes place. When anharmonic decay is rapid, transitions occur before the effects of localization influence diffusion of energy. In this case, $D(\omega)$ is given by $D_h(\omega)$.

We can estimate which diffusion coefficient to use in the regime of localized normal modes, $D_a(\omega)$ or $D_h(\omega)$, for $\omega > \omega_l \approx 150$ cm^{-1}, by calculating the time for a vibrational excitation to diffuse a distance $\xi(\omega)$. This time, t^*, can be estimated as

$$t^*(\omega) = \frac{1}{3}\,\xi^2(\omega)\, D_h{}^{-1}(\omega) \tag{16}$$

where for $D_h(\omega)$ we use eq 13. Then for $\omega > 150$ cm^{-1}, where normal modes are localized, we take the energy diffusion coefficient to be

$$D(\omega) = D_h(\omega), \text{ if } W^{-1}(\omega) \le t^*(\omega) \tag{17a}$$

$$D(\omega) = D_a(\omega), \text{ if } W^{-1}(\omega) > t^*(\omega) \tag{17b}$$

where $t^*(\omega)$ is calculated using eq 16. Equation 17a represents the case where rapid anharmonic decay allows energy diffusion to occur without the restriction of localization, because mode lifetimes are shorter than the time it would take for energy to diffuse the length of the normal mode. We note that in principle, W could be so large as to establish the mean free path, which would then be about $c_s W^{-1}$. However, with $c_s \approx 20$ Å ps^{-1} and $W < 1$ ps^{-1} for thermally accessible modes, the mean free path due to anharmonic decay is greater than the localization length of the modes and so does not influence energy diffusion. Equation 17b represents the case of slow anharmonic decay, which turns out to play a relatively small role in heat flow. In the limit $W = 0$, there is no anharmonic decay of localized modes, and only the extended modes contribute to thermal transport.

At frequencies above the crossover to localization in myoglobin, the localization length decays fairly quickly and is usually 2−5 Å at frequencies above about 500 cm^{-1}. For such short localization lengths, we find t^* using eq 16 to be 1−2 ps, similar to but somewhat shorter than the typical time for anharmonic decay from our calculations, about 2−5 ps. Thus, for $\omega > 500$ cm^{-1}, the energy diffusion coefficient is usually $D_a(\omega)$. However, between the crossover to localization near 150 and 500 cm^{-1}, both $\xi(\omega)$ and $W(\omega)$ are often sufficiently large that eq 17a is satisfied and $D(\omega) \approx D_h(\omega)$. Thus, for most thermally accessible modes, we can approximate $D(\omega) \approx D_h(\omega)$, despite the fact that many of these normal modes are localized. Anharmonic decay of the thermally accessible localized modes is sufficiently rapid for energy to transfer to other modes before localization would influence energy flow.

In Figure 9a, we plot κ, which has been calculated by integrating eq 9 over the full band of frequencies of myoglobin. In the extended regime, i.e., for $\omega < 150$ cm^{-1}, $D(\omega) = D_h(\omega)$, given by eq 13. For $\omega > 150$ cm^{-1}, we calculate $D(\omega)$ using the criterion of eq 17. The localization lengths that enter into the calculation of t^* in eq 16 are those plotted in Figure 3b, and the energy transfer rates, $W(\omega)$, are those plotted in Figure 8 at $T = 135$ K, apart from a correction that we make for the temperature. To account for the temperature variation of $W(\omega)$, we assume that $W(\omega)$ is independent of temperature for $\omega \approx 500$ cm^{-1}, whereas we assume it is proportional to temperature for $\omega < 500$ cm^{-1}, fairly reasonable given the temperature variations we observed in our calculation of $W(\omega)$ at $T = 15$, 45, and 135 K, shown in Figure 8. The value of the thermal

conductivity at 300 K, 2.0 mW cm^{-1} K^{-1}, is almost the same as κ would be, 2.1 mW cm^{-1} K^{-1}, if all normal modes were extended. The thermal conductivity that we have calculated is about one-third the thermal conductivity of H_2O at 300 K, which is 6.1 mW cm^{-1} K^{-1}.[26] At around 300 K, the contributions to thermal conduction in myoglobin from the extended normal modes and from the rapidly decaying localized normal modes are similar, with the latter almost doubling the value of κ_h, the thermal conductivity in the harmonic limit.

The thermal diffusivity of myoglobin can be calculated in terms of κ with eq 10. Results are plotted in Figure 9b from 20 to 320 K. At 300 K, we find the thermal diffusivity of myoglobin to be 14 $Å^2$ ps^{-1}, the same as the value for water.[26] This result is consistent with the 20−30 ps time for heat from a photoexcited heme of myoglobin and hemoglobin to reach the surrounding solvent, measured by Hochstrasser and co-workers,[27] a time scale corroborated by simulations.[28] Our result is also comparable to the thermal diffusivity of 7 $Å^2$ ps^{-1} estimated from a simulated cooling of the photosynthetic reaction center of *Rhodospseudomonas viridis* between 200 and 300 K by Tesch and Schulten.[29]

Because the thermal diffusivities for the protein and water are very close, the discrepancy between their thermal conductivities is largely due to differences in their respective heat capacities. At 300 K, the heat capacity of water is 4.2 J K^{-1} g^{-1}, whereas we calculate the heat capacity of myoglobin to be 1.0 J K^{-1} g^{-1} at 300 K. This latter value is reasonably close to measured heat capacities for proteins. For example, the heat capacity of lysozyme in dilute aqueous solution is 1.5 J K^{-1} g^{-1} and is 1.3 J K^{-1} g^{-1} for the dry protein.[30]

5. Concluding Remarks

We have calculated the coefficient of thermal conductivity and diffusivity for myoglobin over a wide range of temperatures based on calculation of the normal modes, their lifetimes, the speed of sound in the protein, and estimates for the mean free path. We have considered an isolated protein vibrating in a given configuration and used perturbation theory with low-order anharmonic coupling to calculate the lifetimes of the vibrational modes. The large majority of normal modes of myoglobin are localized, essentially all those with frequencies larger than about 150 cm^{-1}. In the harmonic limit, only normal modes extended over the protein can carry heat. In this case thermal diffusion is related to the speed of sound in the protein and mean free path for the extended modes, much as it is in a three-dimensional glass at temperatures above about 20 K.[16−18] At low temperatures, essentially only the low-frequency, extended normal modes of the protein are populated, and the harmonic limit is sufficient for describing thermal transport arising from a modest thermal gradient. However, at higher temperatures such as 300 K, many thermally accessible modes of a protein in the harmonic limit are localized and cannot carry heat, in contrast to a 3D glass. Anharmonicity allows vibrational energy to flow from the localized modes into other modes of the protein. We find that anharmonic decay of thermally accessible localized modes of the protein is usually sufficiently rapid so that effects of localization on heat flow are small.

We have found the thermal diffusivity of myoglobin at 300 K to be 14 $Å^2$ ps^{-1}, the same as that of water, and the coefficient of thermal conductivity to be 2.0 mW cm^{-1} K^{-1}, about one-third the value for water. The thermal diffusivity that we calculate at 300 K is consistent with a value of roughly 15 $Å^2$ ps^{-1} deduced from pump−probe studies on heme proteins[27] and about 7 $Å^2$ ps^{-1} deduced from simulated cooling of *Rps. viridis*.[29] The values that we obtain for the thermal conductivity and diffusivity would be about a factor of 2 smaller if we considered only the harmonic approximation with no anharmonicity, because of localization of thermally accessible normal modes. Moreover, the value of the coefficient continues to rise with temperature for the anharmonic protein, whereas in the harmonic limit it is nearly independent of temperature by 300 K.

We have shown that two localized modes whose centers of excitation are close in space tend to have quite different frequencies, i.e., localized modes at higher frequencies appear to "repel" one another. Modes with similar frequencies rarely overlap in space, which influences the rate of anharmonic decay of high-frequency, localized modes. Anharmonic matrix elements coupling, for example, two high-frequency modes and a low-frequency mode are usually small because of mode repulsion, and energy transfer from a high-frequency mode to a mode of similar frequency and the remainder to low-frequency modes often occurs very slowly. Energy transfers preferably to modes of intermediate frequencies provided resonances are available. As a result, lifetimes of higher frequency modes are typically only weakly dependent on temperature. This trend is consistent with the nearly temperature-independent anharmonic decay rates of high-frequency modes in both myoglobin[3] and myoglobin-CO[24,25] found in pump−probe studies over temperature ranges spanning about 300 K.

The present study has focused on heat transport and anharmonic decay in the protein alone. Solvent modes also play an important role in vibrational energy transfer, particularly at lower frequencies. Below 300 cm^{-1} and in some cases at higher frequency, many vibrational modes cannot be distinguished as belonging to the protein or solvent. Future work will examine the role of these strongly mixed modes in vibrational energy transfer and heat flow.[31]

Acknowledgment. This work was supported by the National Science Foundation (NSF CHE-0112631), by a New Faculty Award from the Camille and Henry Dreyfus Foundation, and by a Research Innovation Award from the Research Corporation.

References and Notes

(1) Hamm, P.; Lim, M.; Hochstrasser, R. M. *J. Phys. Chem. B* **1998**, *102*, 6123.

(2) Xie, A.; van der Meer, L.; Hoff, W.; Austin, R. H. *Phys. Rev. Lett.* **2000**, *84*, 5435.

(3) Peterson, K. A.; Rella, C. W.; Engholm, J. R.; Schwettman, H. A. *J. Phys Chem. B* **1999**, *103*, 557.

(4) Nishikawa, T.; Go, N. *Proteins: Struct., Funct., Genet.* **1987**, *2*, 308.

(5) Seno, Y.; Go, N. *J. Mol. Biol.* **1990**, *216*, 111.

(6) Levitt, M.; Sander, C.; Stern, P. S. *J. Mol. Biol.* **1985**, *181*, 423.

(7) McCammon, J. A.; Harvey, S. C. *Dynamics of Proteins and Nucleic Acids*; Cambridge University Press: Cambridge, 1987.

(8) Brooks, C. L.; Karplus, M.; Pettitt, B. M. *Adv. Chem. Phys.* **1988**, *71*, 1.

(9) Roitberg, A.; Gerber, R. B.; Elber, R.; Ratner, M. A. *Science* **1995**, *268*, 1319. Roitberg, A.; Gerber, R. B.; Ratner, M. A. *J. Phys. Chem. B* **1997**, *101*, 1700.

(10) Moritsugu, K.; Miyashita, O.; Kidera, A. *Phys. Rev. Lett.* **2000**, *85*, 3970.

(11) Leitner, D. M. *Phys. Rev. Lett.* **2001**, *87*, 188102.

(12) Leitner, D. M. *J. Phys. Chem. A* **2002**, *106*, 10870.

(13) Matsuda, H.; Ishii, K. *Suppl. Prog. Theor. Phys.* **1970**, *45*, 56.

(14) Fabian, J. *Phys. Rev. B* **1997**, *55*, R3328.

(15) Leitner, D. M. *Phys. Rev. B* **2001**, *64*, 094201.

(16) Fabian, J.; Allen, P. B. *Phys. Rev. Lett.* **1997**, *79*, 1885. Allen, P. B.; Feldman, J. L.; Fabian, J.; Wooten, F. *Philos. Mag. B* **1999**, *79*, 1715.

(17) Taraskin, S. N.; Elliott, S. R. *Phys. Rev. B* **2000**, *61*, 12017; 12031.
(18) Sheng, P.; Zhou, M.; Zhang, Z. Q. *Phys. Rev. Lett.* **1994**, *72*, 234.
(19) Alexander, S.; Entin-Wohlman, O.; Orbach, R. *Phys. Rev. B* **1986**, *34*, 2726. Jagannathan, A.; Orbach, R.; Entin-Wohlman, O. *Phys. Rev. B* **1989**, *39*, 13465.
(20) Michalski, J. *Phys. Rev. B* **1992**, *45*, 7054.
(21) Elber, R.; et al. *Comput. Phys. Commun*. **1995**, *91*, 159. The version used for this study was obtained from http://www.tc.cornell.edu/reports/NIH/resource/CompBiologyTools/moil.
(22) Bell, R. J.; Dean, P. *Discuss. Faraday Soc.* **1970**, *50*, 55.
(23) Maradudin, A. A.; Fein, A. E. *Phys. Rev.* **1962**, *128*, 2589.
(24) Rella, C. W.; Rector, K. D.; Kwok, A.; Hill, J. R.; Schwettman, H. A.; Dlott, D. D.; Fayer, M. D. *J. Phys. Chem.* **1996**, *100*, 15620.
(25) Fayer, M. D. *Annu. Rev. Phys. Chem.* **2001**, *52*, 315.
(26) Lide, D. R., Ed. *CRC Handbook of Chemistry and Physics;* 71st ed.; CRC Press: Boca Raton, FL, 1992.
(27) Lian, T. Q.; Locke, B.; Kholodenko, Y.; Hochstrasser, R. M. *J. Phys. Chem.* **1994**, *98*, 11648.
(28) Sagnella, D. E.; Straub, D. E.; Thirumalai, D. *J. Chem. Phys.* **2000**, *113*, 7702.
(29) Tesch, M.; Schulten, K. *Chem. Phys. Lett.* **1990**, *169*, 97.
(30) Yang, P.-H.; Rupley, J. A. *Biochemistry* **1979**, *18*, 2654.
(31) Yu, X.; Leitner, D. M. (in preparation).